



Published in final edited form as:

*Cell Transplant.* 2015 ; 24(9): 1687–1698. doi:10.3727/096368914X684619.

## Mesenchymal stromal cells improve renovascular function in Polycystic Kidney Disease

Federico Franchi, PhD<sup>1</sup>, Karen M. Peterson, BS<sup>1</sup>, Rende Xu, MD<sup>1</sup>, Brent Miller<sup>1</sup>, Peter J Psaltis, MD<sup>1,2</sup>, Peter C. Harris, PhD<sup>3</sup>, Lilach O. Lerman, MD<sup>3</sup>, and Martin Rodriguez-Porcel, MD<sup>1</sup>

<sup>1</sup>Division of Cardiovascular Diseases, Department of Internal Medicine, Mayo Clinic, Rochester, MN, USA

<sup>2</sup>Department of Medicine, University of Adelaide, Adelaide, Australia

<sup>3</sup>Division of Nephrology and Hypertension, Department of Internal Medicine, Mayo Clinic, Rochester, MN, USA

### Abstract

Polycystic kidney disease (PKD) is a common cause of end stage renal failure, for which there is no accepted treatment. Progenitor and stem cells have been shown to restore renal function in a model of renovascular disease, a disease that shares many features with PKD. The objective of this study was to examine the potential of adult stem cells to restore renal structure and function in PKD.

Bone marrow-derived mesenchymal stromal cells (MSCs,  $2.5 \times 10^5$ ) were intrarenally infused in 6 week-old PCK rats. At 10 weeks of age, PCK rats had an increase in systolic blood pressure (SBP) vs. controls ( $126.22 \pm 2.74$  vs.  $116.45 \pm 3.53$  mmHg,  $p < 0.05$ ) and decreased creatinine clearance ( $3.76 \pm 0.31$  vs.  $6.10 \pm 0.48$   $\mu\text{l}/\text{min}/\text{g}$ ,  $p < 0.01$ ), which were improved in animals that received MSCs (SBP:  $114.67 \pm 1.34$  mmHg, and creatinine clearance:  $4.82 \pm 0.24$   $\mu\text{l}/\text{min}/\text{g}$ ,  $p = 0.001$  and  $p = 0.003$  vs. PKD, respectively). MSCs preserved vascular density and glomeruli diameter, measured using micro-computed tomography. PCK animals had increased urine osmolality ( $843.9 \pm 54.95$  vs.  $605.6 \pm 45.34$  mOsm,  $p < 0.01$  vs. control), which was improved after MSC infusion and not different from control ( $723.75 \pm 56.6$  mOsm,  $p = 0.13$  vs. control). Furthermore, MSCs reduced fibrosis and preserved the expression of the pro-angiogenic molecules, while cyst size and number were unaltered by MSCs.

Delivery of exogenous MSCs improved vascular density and renal function in PCK animals, and the benefit was observed up to four weeks after a single infusion. Cell-based therapy constitutes a novel approach in PKD.

### Keywords

polycystic kidney disease; mesenchymal stromal cells; vasculature; renal function; kidney

Corresponding author: Martin Rodriguez-Porcel, MD, 200 First St SW, Rochester, MN 55905, Phone: 507-284-4442, Fax: 507-266-0228, rodriguez.m@mayo.edu.

**Disclosure:** The authors have no conflicts to disclose pertaining to this manuscript.

## Introduction

Hereditary PKD is one of the most common lethal monogenic genetic diseases of man, affecting ~1/1,000 individuals, and constitutes a common cause of end stage renal disease (ESRD) (38,40). PKD can be divided into autosomal dominant PKD (ADPKD) and autosomal recessive PKD (ARPKD). Either of two loci *PKD1* or *PKD2*, encoding polycystin-1 and -2, respectively can cause ADPK; while *PKHD1*, encoding fibrocystin, is the ARPKD locus. These proteins are ciliary glycoproteins, thought to regulate renal tubular (40) and vascular development (14,28,33). AD- and AR-PKD are considered to mainly affect tubular cells in the collecting duct, leading to the formation of parenchymal cysts with subsequent tubular and renal dysfunction, and ultimately ESRD. However, the abnormalities in PKD extend beyond cyst development and renal tubular dysfunction, as around 50% of patients with ADPKD develop hypertension and vascular dysfunction, with hypertension also being common in ARPKD (3,6,13). Furthermore, we recently showed that the ARPKD rat model (PCK) (15) is associated with decreased renal vascular density what could be partly responsible for the decrease in renal function observed in these animals (48). Despite increasing knowledge of the pathophysiology of PKD, no approved treatments are yet available to slow the progression of renal dysfunction.

Recently, the use of progenitor or stem cells has attracted significant interest in many renal diseases (11,41). In fact, our group has successfully used progenitor and stem cells to restore renal function in an experimental model of renovascular disease (RVD), a disease that is also characterized by alterations in vascular and tubular structure and function (4,5,7,50). In those studies, a single intrarenal infusion of mesenchymal stromal cells (MSCs) or endothelial progenitor cells during the evolution of RVD restored the hemodynamics and functions of the ischemic kidney, preserved microvascular architecture, and attenuated renal remodeling.

Thus, keeping in mind the pathological differences between RVD and PKD, but at the same time focusing on the similarities that these two models share in renovascular dysfunction, the present study tested the hypothesis that a single intrarenal infusion of MSCs would blunt the progression of renal dysfunction in PKD.

## Methods

### Experimental Design

All procedures were approved by the Institutional Animal Care and Use Committee. Female rats were divided into wild type controls (Sprague-Dawley), PKD (PCK rat model) (15) and PKD+MSCs (n=10 each). At 6 weeks of age, the PCK animals received an intra-renal infusion of bone-marrow derived MSCs and were subsequently followed for 4 weeks. SBP was assessed non-invasively using the tail cuff method at 6 weeks and weekly thereafter for the duration of the study. For the measurement of sodium excretion and urine osmolality we performed studies in metabolic cages (24 hour) at 6 and 10 weeks of age. Blood samples were obtained at time of euthanasia and tissue prepared for ex vivo analysis. At the end of the study, some kidneys (n=6 per group) were prepared for mCT analysis of the vasculature.

## Stem cell harvesting, characterization, and delivery

MSCs were isolated from the bone marrow of 5-week old wild type male Sprague-Dawley rats and characterized for expression of CD90 and CD29, and negative expression for CD45 and CD11b/c, as previously described by our group (24). At 6 weeks of age, animals were anesthetized with 5% isoflurane (Cardinal Health, Lakeland, FL, USA) on 1 L/min O<sub>2</sub> and maintained with 1–2% isoflurane. Through a small midline incision the proximal part of the left renal artery was exposed and carefully isolated from the renal vein. For cell delivery, a very small needle (33G, Cadence, Inc., Staunton, VA, USA) was used to deliver either MSCs (passage 10,  $2.5 \times 10^5$  in 250  $\mu$ l of PBS, Life Technologies, Grand Island, NY, USA) or saline (250  $\mu$ l of PBS), via the proximal renal artery. The needle was then removed, an absorbable gelatin sponge (Ethicon, Inc., Somerville, NJ, USA) used to prevent bleeding and the abdominal incision was then closed in two layers: muscle using a 4-0 silk suture (Cardinal Health) and skin using a 4-0 absorbable vicryl suture (Cardinal Health).

## In vivo studies

**Blood pressure measurements**—Conscious animals were trained to the tail cuff (Kent Scientific, Torrington, CT, USA) for 1 week prior to blood pressure measurements. On the day of the studies, a cuff was placed around the animal's tail to obtain mean SBP readings, using the CODA blood pressure measurement system (Kent Scientific) (8,47,48).

**Glomerular function**—Creatinine levels in blood and urine as well as proteinuria was measured as previously described (48).

**Renal tubular function**—Studies in metabolic cages (24 hours periods) were performed at baseline (week 6) and 4 weeks after the delivery of stem cells. Sodium and potassium concentration was determined using the EasyLyte Lithium Analyzer (Medica Corp, Bedford, MA, USA), and daily sodium excretion calculated as sodium concentration  $\times$  daily urine volume. Urine osmolality was measured and expressed as mOsmol (Osmometer 3250, Advanced Instruments Inc., Norwood, MA, USA).

**Imaging of transplanted MSCs**—Molecular imaging studies were conducted to ascertain that most of the transplanted MSCs remained in the delivered kidney. For this purpose, rat MSCs were transfected using Effectene Transfection Reagent (Qiagen, Inc., Valencia, CA, USA) according to manufacturer instructions. Cells ( $6 \times 10^5$ ) were plated in 10 cm dishes (Sarstedt, Inc., Newton, NC, USA) and transfected 24 hours later with 5  $\mu$ g of CMV-Fluc plasmid (a plasmid carrying the firefly luciferase gene driven by a cytomegalovirus promoter), kindly provided by Dr. Ian Chen of Stanford University. Then, transfected MSCs were infused in two separate animals following the protocol previously described in the Methods section. Optical bioluminescence imaging was performed 24 hours after transplantation using a cooled charged-couple device camera (Xenogen, Caliper LS, Perkin Elmer, Waltham, MA, USA). After intraperitoneal injection of the reporter substrate D-Luciferin (375 mg/kg of body weight), rats were imaged for 30 minutes using 5-minute acquisition scans and displayed.

To confirm that MSCs remained in the kidney for the duration of follow-up, in a separate set of animals (n=6), the infused cells were labeled prior to infusion with the fluorescent marker CM-DiI (Cell Tracker CM-DiI, Invitrogen, Grand Island, NY, USA; 4 $\mu$ M). Briefly, MSCs were rinsed in PBS and incubated for 20 min at 37°C in 4  $\mu$ M CM-DiI. The solution was then removed and the cells washed twice with PBS and prepared for injection.

Four weeks after transplantation, renal tissue was harvested and examined under a fluorescence microscope.

### Ex vivo studies

**Micro-computed tomography**—mCT tissue preparation was performed as previously described from our laboratory (32,48). After scanning, the 3D volume images were reconstructed with a modified Feldkamp's filtered back projection algorithm, displayed with a cubic voxel of 17  $\mu$ m, and the radio-opacity of each voxel represented by a 16-bit gray-scale value. Image analysis was then performed with the Analyze™ software package (Biomedical Imaging Resource, Mayo Foundation, Rochester, MN, USA).

**Vasculature:** As previously described, the cortex was divided into outer and inner regions, and the outer medulla into an outer and inner strip (23,48). The spatial density of cortical microvessels (diameters <200  $\mu$ m) was calculated in each cross-section. Microvessels were further classified as small (diameters between 18 and 99  $\mu$ m), medium (diameters between 100 to 199  $\mu$ m) and large microvessels (>200  $\mu$ m). The VVF in each renal region was also calculated from their cross-sectional slices as previously described. (23,48).

**Glomeruli:** For glomerular quantification, the analysis was performed as previously described (48). Briefly, the entire renovascular tree was tomographically connected and the glomeruli tomographically isolated using an intensity threshold that converted the image into a binary image. Then the glomeruli were counted using Matlab® software (MathWorks, Natick, MA, USA), and expressed as number of glomeruli per mm<sup>3</sup>.

**Cyst volume:** After creating 3D volume renderings of the cysts, binary images were created to identify renal cysts, and then calculate their cross sectional areas and the entire kidney cyst number.

### Tissue analysis

**Histological analysis:** Renal tissues were fixed in 10% neutral buffered formalin (Fisher Scientific, Pittsburgh, PA, USA), dehydrated and embedded in paraffin and histologic sections (4 $\mu$ m thick) were prepared. Representative slides were stained with hematoxylin & eosin (H&E, Richard-Allan Scientific Co, Kalamazoo, MI, USA) to assess the renal morphology and the development of cysts, and Picrosirius Red (American MasterTech, Lodi, CA, USA) to evaluate fibrosis. To examine the presence of pro-angiogenic cytokines, additional unstained slides were prepared for immunohistochemical staining for VEGF-A (Novus Biological, Littleton, CO, USA; dilution 1:50). All the stainings were imaged using a Nikon Eclipse 50i clinical microscope (Nikon Instruments Inc., Melville, NY, USA) and Spot Advanced modular image software (Spot™ Imaging Solutions, Sterling Heights, MI,

USA). Quantitative analysis was performed using MetaMorph microscopy automation and image analysis software (Molecular Devices, LLC, Sunnyvale, CA, USA) and averaged from four random fields of view ( $\times 20$  magnification) for each of the cortex and medulla per slide, per animal.

For the MSCs-labeling studies, renal tissues were flash frozen and observed under a fluorescent microscope (LSM 510 Confocal Laser Scanning Microscope, Carl Zeiss MicroImaging, Inc. Oberkochen, Germany). CM-DiI staining was imaged using an excitation wavelength of 534 nm and an emission wavelength of 560 nm. DAPI (Life Technologies) was used as a nuclear counterstain (using excitation and emission wavelengths of 405 and 420–460 nm, respectively) (31). Images were obtained at a magnification of  $20\times$ . To characterize the phenotype of the transplanted cells, CM-DiI-labeled MSCs were co-stained with vWf (Abcam, dilution 1:400) as a marker of endothelial phenotype or pan cytokeratin (Genway Biotech Inc, San Diego, CA, USA, dilution 1:100) as a marker of epithelial (tubular) phenotype.

**Western blotting:** Protein expression was evaluated by western blotting. Total lysate protein concentration was determined using the Bradford Assay (Bio-Rad, Hercules, CA, USA) and 25  $\mu\text{g}$  protein per sample were loaded onto 10% PAGE gels (Bio-Rad), electrophoresed for 90 min at 90V in Tris-glycine-SDS buffer (Bio-Rad), then transferred to PVDF membranes (Bio-Rad) in Tris-glycine-SDS plus 20% methanol (Sigma-Aldrich, St. Louis, MO, USA) at 12 V for one hour in a TE70X semi-dry transfer apparatus (Hoefer, Inc., Holliston, MA, USA). Membranes were blocked for one hour in Tris-Buffered Saline Tween-20 (TBST, Bio-Rad) containing 5% milk (TBST:milk) followed by overnight incubation on rocker at  $4^{\circ}\text{C}$  with primary antibodies diluted in TBST:milk. Following incubation with primary antibody, membranes were washed once for 5 minutes, then 3 times for 10 minutes each in TBST and then incubated on rocker for one hour at room temperature with horseradish peroxidase conjugated secondary antibody diluted (Santa Cruz Biotechnology, Santa Cruz, CA, USA) in TBST:milk. Wash steps were repeated as above, and then membranes were incubated for 5 min. with SuperSignal West Pico Chemiluminescent Substrate (Thermo Scientific, Rockford, IL, USA), per manufacturer's instructions and imaged by film (Denville Scientific, Inc., Metuchen, NJ, USA) exposure. Band densities were analyzed by ImageJ (NIH, Bethesda, MD, USA) and normalized to corresponding loading control band densities. Rabbit anti- $\beta$ -actin (Abcam, Cambridge, MA, 1:5000) was used as loading control. Primary antibodies included HIF-1 $\alpha$  (Abcam, dilution 1:1000), VEGF receptor 1 (VEGFR1, Abcam, dilution 1:10000), VEGF-A (Abcam, dilution  $1\mu\text{g}/\text{ml}$ ).

### Statistical Analysis

Data are expressed as mean $\pm$ SEM. Statistical comparisons between the groups were performed using ANOVA and the Bonferroni post-hoc test, when applicable. Statistical significance was established at two-tailed  $p < 0.05$ .

## Results

### Characteristics of PKD and control animals

At 6 weeks of age, there were no significant differences in systolic blood pressure (SBP) between PCK and control ( $113.81 \pm 2.83$  vs.  $108.38 \pm 2.76$  mmHg, respectively,  $p=0.16$ ) and protein/creatinine ratio ( $0.92 \pm 0.18$  vs.  $0.69 \pm 0.04$ , respectively,  $p=0.11$ ). However, the clearance of creatinine (CrCl) was lower in PCK animals than in control (control:  $2.61 \pm 0.20$  vs. PCK:  $1.75 \pm 0.26$   $\mu\text{l}/\text{min}/\text{g}$  of body weight,  $p<0.05$ ) and urine osmolality increased (control:  $346.6 \pm 56.70$  vs. PCK:  $682.3 \pm 61.04$  mOsm/day,  $p<0.001$ ). Therefore, at the time point when MSCs were infused, the PCK animals already demonstrated renal dysfunction.

Moreover, compared to controls, 10 week-old PKD animals (4 weeks after MSCs delivery) had an increase in SBP (Figure 1A), increase body weight ( $190.40 \pm 3.13$  vs.  $209.40 \pm 8.33$  grams,  $p<0.05$ ), and a more profound decrease in renal function, with an increase in protein/creatinine ratio (control:  $0.48 \pm 0.06$ , PCK:  $1.33 \pm 0.39$ ,  $p<0.05$ ), and a decrease in CrCl (Figure 1B). In metabolic studies PCK animals also showed an increase in urine osmolality (Figure 1C) and decreased sodium excretion compared to control (control:  $0.80 \pm 0.07$  vs. PCK:  $0.43 \pm 0.08$  mEq/day,  $p<0.001$ ).

As in our prior study, the PCK animals had a decrease in vascular density in both the cortex and medulla (Figure 2A and B), as measured by micro-computed tomography (mCT). This decrease was mostly due to vessels under  $200\mu\text{m}$  in diameter, along with a decrease in vascular volume fraction (VVF) that was most prominent in the inner cortex (Table). The PCK animals also showed glomerular hypertrophy although the number of glomeruli remained unchanged (Table). In ex vivo studies, 10 week-old PCK animals showed development of cysts (Figure 3A) and increased fibrosis, compared to control, both in the cortex and the medulla (Figure 3B), as measured by Picosirius red. Western blotting and immunohistochemical staining also revealed a decreased expression of vascular endothelial growth factor (VEGF) pathway proteins and hypoxia inducible factor (HIF)-1 $\alpha$  in PCK animals compared to control (Figure 4A and B).

### Effect of MSCs in ARPKD

At 10 weeks (4 weeks after MSCs or placebo delivery), the PCK rats that received MSCs had levels of SBP comparable to control and lower than without treatment (Figure 1A), while there was no difference in the body weight between PCK and PCK+MSCs ( $209.71 \pm 3.60$  grams,  $p=\text{NS}$ ). Importantly, while the CrCl was not normalized in PCK+MSCs, it was significantly improved compared to PCK (Figure 1B), although the protein/creatinine ratio did not change (PCK+MSCs:  $0.83 \pm 0.13$ ,  $p=0.34$  vs. PCK). MSCs also improved urine osmolality, a parameter of renal tubular function (Figure 1C), without significant changes in sodium excretion ( $0.39 \pm 0.06$  mEq/day,  $p=0.33$  vs. PCK and  $p<0.01$  vs. control).

A single intra-renal artery delivery of MSCs improved the cortical vascular density in the PCK animals, a beneficial effect that was maintained 4 weeks after treatment (Figure 2A and B). The improvement in cortical density was observed in both the inner and outer cortex (Figure 2B), due to preservation of vessel density under  $200\mu\text{m}$ , together with an

improvement in inner cortical VVF (Table). There was also improvement in medullary vascular density in animals treated with MSCs (Figure 2B). Furthermore, animals that received MSCs also showed normalization of glomerular diameter (Table). On the other hand, compared to PCK, PCK+MSCs had similar cyst size ( $5.5\pm 0.7\text{ mm}^3$  and  $4.9\pm 0.5\text{ mm}^3$ ,  $p=0.24$ ) and number ( $36.2\pm 8.1$  and  $37.8\pm 4.5$ ,  $p=0.43$ ), as well as similar percentage of renal volume occupied by cysts ( $9.2\pm 1.8$  and  $9.6\pm 0.9\%$ ,  $p=0.34$ ).

In PCK animals that received MSCs the degree of fibrosis was significantly decreased compared to PCK and similar to control (Figure 3B). Furthermore, MSCs partially preserved the expression of VEGF and HIF 1- $\alpha$  in the PCK animals (Figure 4A and B).

### Safety and status of MSCs after transplantation

The infusion of MSCs through the renal artery was safe, and no mortality was observed in the protocol used in this study. Furthermore, we observed that MSCs remained in the infused kidney with no detectable spill-over after delivery (Figure 5A). At three days post-delivery, the MSCs mostly localized in the glomeruli (Figure 5B and C), while only a few were retained in the interstitial space (Figure 5D and E). In fact, even four weeks after infusion, MSCs labeled with the fluorescent marker CM-DiI were detected mainly in the glomeruli, with some expressing the endothelial marker vonWillebrand factor (vWF; Figure 5F). We were also able to observe the presence of sporadic MSCs in the renal tubulo-interstitial compartment, some of which expressed pan-cytokeratin, a marker of an epithelial phenotype (Figure 5G).

### Discussion

This study shows that a single infusion of MSCs preserved SBP and partially restored renal function in this PKD model. We found that MSCs improved vascular density, both in the cortex and the medulla, despite no changes in cyst size. Furthermore, 4 weeks after transplantation, a portion of the MSCs that remained in the kidney acquired endothelial and/or tubular characteristics.

PKD is a common cause of ESRD and significant advances have been made in understanding its pathogenesis (38). Several studies have linked PKD and renal tubular dysfunction, indicating that at the different stages of PKD, the renal concentrating ability and tubular function are abnormal. Several clinical studies have tested novel interventional strategies focused on the modulation of renal tubular function (9,37,49). However, so far, the outcome of these studies has been inconclusive (39). Thus, novel approaches in the treatment of PKD are needed to provide novel insights on the disease and potentially novel therapeutic approaches that could complement strategies currently under investigation.

In addition to abnormalities in tubular function (38), a significant number of PKD patients suffer from hypertension and vascular derangements like intracranial aneurysms, conditions that are significant causes of morbidity and mortality in patients with PKD (6). Previous studies have also reported that PKD is associated with a dysregulation of nitric oxide and abnormal endothelial function (43,44). Furthermore, we have recently shown that the PKD kidney has decreased renal perfusion and glomerular function, characterized by reduced

clearance of creatinine and increased protein/creatinine ratio (48). In this study we also show that the PCK animals have a decrease in daily sodium excretion, which may increase blood volume, potentially contributing to the hypertension seen in PKD. Taken together, these studies showed that PKD is characterized not only by changes in tubular function, but also by changes in vascular structure and function, potentially representing a novel therapeutic target for this disease.

Regenerative medicine has appeared as a novel therapeutic strategy for many renal diseases (10). Within the many reparative cell alternatives available, MSCs have attracted special attention due to their ease of isolation and maintenance, together with the fact that they do not trigger a significant immune response (25,27). In this study we show, for the first time, the potential of stem cells for the treatment of PKD, showing that a single infusion of MSCs normalized blood pressure and resulted in an improvement in vascular and, to some extent, tubular function.

The improvement in vascular density was seen in both the cortical and medullary region. Furthermore, this improvement was seen mainly on the small microvessels (under 200 $\mu$ m in diameter), which are largely responsible for vascular resistance (18) that can explain the better blood pressure regulation in these animals. Importantly, restoration of the microvasculature, despite no changes in the cyst size or number, was capable of improving renal and tubular function in this model of PKD. This may suggest that some of the renal functional decline in this model may be, in part, secondary to microvascular rarefaction, and provides the rationale for strategies to restore vascular density and function. Based on the observation that glomeruli number is not affected in this model of PKD, it is possible that the vessels affected are not those leading to glomeruli function but rather those that have other vascular functions.

Importantly, MSCs also preserved vascular density both in the outer and inner medulla, despite the lack of change in cyst size and/or number, suggesting that these changes may be independent, at least in part, from a physical impact of cysts on the medullary tissue. The lack of improvement seen in medullary VVF can be explained by a previously described autoregulatory mechanism involving oxidative stress in the medullary thick ascending limb of Henle (17,21). Alternatively, this phenomenon could be related to the persistence of pre-existing cysts in that region of the kidney, which may not allow for vessels to fully develop in the medullary tissue, limiting the impact vessels will have on VVF calculation. That being said, further studies should focus on the interaction between vessels and cyst development.

We were able to detect MSCs both in the glomeruli and tubules after cell infusion. In fact, numerous studies have recently reported the engraftment of MSCs in acute renal injury models. However, while some of them showed glomerular as well as tubular distribution (12,20), others did not observe engraftment into vessels and glomeruli, but only in the tubular compartment, either promoting higher proliferation of surviving epithelial tubular cells (29) or differentiating into tubular epithelial cells (22). In this regard, we must take into account the morphological and physiological characteristics of different disease models that may play an important role in engraftment, survival and differentiation capacity of transplanted stem cells. Furthermore, considering that PKD is a chronic disease with a



repetitive and continuous insult to the vasculature, we believe that sustained cell survival will be important to the beneficial effect of these therapies, as increased cell survival likely means sustained cytokine release, leading to a larger beneficial effect.

MSCs have been shown to exert mainly paracrine effects (1,16,36), by releasing a number of cytokines, such as SDF1, VEGF and HGF, leading to a vast array of beneficial effects, mainly on the vasculature of the treated organ, which may have pro-angiogenic and anti-inflammatory effects, also leading to decreased fibrosis. In this study we also show that, after transplantation, MSCs can acquire characteristics of endothelial cells, suggesting that some transplanted MSCs can transdifferentiate. The transdifferentiation potential of stem cells observed is supported by reports using endothelial progenitor cells in an animal model of renovascular disease (4). Although the extent of the beneficial effect that the transdifferentiated MSCs have in the PKD kidney remains unclear, it does speak of the plasticity of these cells that can acclimate to different microenvironments. Future studies are needed to clearly identify the mechanisms driving this beneficial effect of MSCs in PKD.

Most studies have shown that cells have poor survival after transplantation (30,31,42), leading to significant interest in the monitoring of the viability of these cells over time (2). For this purpose, we and others have used reporter genes strategies to locate and quantify the survival of cells transplanted to different organs/systems (26,30,31,34,35,42,45). In this study we show that MSCs persist in the kidney for the duration of the study, providing evidence that retention of transplanted cells in the infused kidney may be better than the retention seen in other organs, like the heart. In future studies our group will focus on the retention rate and survival of transplanted cells in PKD.

### Limitations

this study used a single dose of stem cells that, in a disease characterized by a continuous deleterious insult/noxious microenvironment, may have finite or limited effect. Future studies are needed to evaluate the beneficial effect of repetitive infusion or different doses of MSCs. The results of this study are limited to a 4-week follow-up and further studies should be done to examine the duration of the beneficial effect.

MSCs did not change the number or size of PKD cysts. This is not surprising as the development of cysts is likely the result of the genetic defect in fibrocystin unlikely to be reversed by a single dose and infusion of MSCs. Nevertheless, it is very encouraging that one single dose of MSCs lead to a significant beneficial effect on the vasculature and that benefits were maintained up to 4 weeks post single treatment.

In this study we used a rat PCK model of PKD that has been extensively used to test other therapeutic alternatives (15,19,46,48). Although is a genetic model of ARPKD, it has been shown to share many features with ADPKD, the adult and most common form of PKD (15). Furthermore, it provides further evidence that the PCK rat model of PKD shares many vascular features with ADPKD, suggesting that this model may be used to test novel interventions for PKD.

## Clinical Perspective

this study describes the potential for the use of stem cells for the treatment of PKD, providing a new paradigm for the treatment of this disease. Our results may serve to prompt evaluation of the potential adjuvant role of cell therapy in a genetic disease like PKD, which can be complemented with other therapeutic strategies currently under investigation.

## Acknowledgements

The authors want to acknowledge Dr. Xiaofang Wang for her assistance with the PCK model and Mr. Bruce Knudsen for the assistance with the non-invasive measurement of blood pressure.

Funding: National Institutes of Health grants DK 90728 and HL88048, and the Mayo Foundation.

## Bibliography

1. Afzal MR, Haider H, Idris NM, Jiang S, Ahmed RP, Ashraf M. Preconditioning promotes survival and angiomyogenic potential of mesenchymal stem cells in the infarcted heart via NF-kappaB signaling. *Antioxid. Redox Signal.* 2010; 12(6):693–702. [PubMed: 19751147]
2. Buxton DB, Antman M, Danthi N, Dilsizian V, Fayad ZA, Garcia MJ, Jaff MR, Klimas M, Libby P, Nahrendorf M, Sinusas AJ, Wickline SA, Wu JC, Bonow RO, Weissleder R. Report of the National Heart, Lung, and Blood Institute working group on the translation of cardiovascular molecular imaging. *Circulation.* 2011; 123(19):2157–2163. [PubMed: 21576680]
3. Cadnapaphornchai MA, McFann K, Strain JD, Masoumi A, Schrier RW. Increased left ventricular mass in children with autosomal dominant polycystic kidney disease and borderline hypertension. *Kidney Int.* 2008; 74(9):1192–1196. [PubMed: 18716604]
4. Chade AR, Zhu X, Lavi R, Krier JD, Pislaru S, Simari RD, Napoli C, Lerman A, Lerman LO. Endothelial progenitor cells restore renal function in chronic experimental renovascular disease. *Circulation.* 2009; 119(4):547–557. [PubMed: 19153272]
5. Ebrahimi B, Eirin A, Li Z, Zhu XY, Zhang X, Lerman A, Textor SC, Lerman LO. Mesenchymal stem cells improve medullary inflammation and fibrosis after revascularization of swine atherosclerotic renal artery stenosis. *PloS One.* 2013; 8(7):e67474. [PubMed: 23844014]
6. Ecker T, Schrier RW. Cardiovascular abnormalities in autosomal-dominant polycystic kidney disease. *Nat. Rev. Nephrol.* 2009; 5(4):221–228. [PubMed: 19322187]
7. Eirin A, Zhu XY, Krier JD, Tang H, Jordan KL, Grande JP, Lerman A, Textor SC, Lerman LO. Adipose tissue-derived mesenchymal stem cells improve revascularization outcomes to restore renal function in swine atherosclerotic renal artery stenosis. *Stem Cells.* 2012; 30(5):1030–1041. [PubMed: 22290832]
8. Feng M, Whitesall S, Zhang Y, Beibel M, D'Alecy L, DiPetrillo K. Validation of volume-pressure recording tail-cuff blood pressure measurements. *Am. J. Hypertension.* 2008; 21(12):1288–1291.
9. Hoher B, Kalk P, Slowinski T, Godes M, Mach A, Herzfeld S, Wiesner D, Arck PC, Neumayer HH, Nafz B. ETA receptor blockade induces tubular cell proliferation and cyst growth in rats with polycystic kidney disease. *J. Am. Soc. Nephrol.* 2003; 14(2):367–376. [PubMed: 12538737]
10. Hopkins C, Li J, Rae F, Little MH. Stem cell options for kidney disease. *J. Pathol.* 2009; 217(2): 265–281. [PubMed: 19058290]
11. Ikarashi K, Li B, Suwa M, Kawamura K, Morioka T, Yao J, Khan F, Uchiyama M, Oite T. Bone marrow cells contribute to regeneration of damaged glomerular endothelial cells. *Kidney Int.* 2005; 67(5):1925–1933. [PubMed: 15840040]
12. Imasawa T, Utsunomiya Y, Kawamura T, Zhong Y, Nagasawa R, Okabe M, Maruyama N, Hosoya T, Ohno T. The potential of bone marrow-derived cells to differentiate to glomerular mesangial cells. *J. Am. Soc. Nephrol.* 2001; 12(7):1401–1409. [PubMed: 11423569]
13. Kelleher CL, McFann KK, Johnson AM, Schrier RW. Characteristics of hypertension in young adults with autosomal dominant polycystic kidney disease compared with the general U.S. population. *Am. J. Hypertension.* 2004; 17(11 Pt 1):1029–1034.

14. Kim K, Drummond I, Ibraghimov-Beskrovnaya O, Klinger K, Arnaout MA. Polycystin 1 is required for the structural integrity of blood vessels. *Proc. Natl. Acad. Sci. USA.* 2000; 97(4): 1731–1736. [PubMed: 10677526]
15. Lager DJ, Qian Q, Bengal RJ, Ishibashi M, Torres VE. The pck rat: a new model that resembles human autosomal dominant polycystic kidney and liver disease. *Kidney Int.* 2001; 59(1):126–136. [PubMed: 11135065]
16. Liu SH, Huang JP, Lee RK, Huang MC, Wu YH, Chen CY, Chen CP. Paracrine factors from human placental multipotent mesenchymal stromal cells protect endothelium from oxidative injury via STAT3 and manganese superoxide dismutase activation. *Biol. Reprod.* 2010; 82(5):905–913. [PubMed: 20107204]
17. Makino A, Skelton MM, Zou AP, Roman RJ, Cowley AW Jr. Increased renal medullary oxidative stress produces hypertension. *Hypertension.* 2002; 39(2 Pt 2):667–672. [PubMed: 11882628]
18. Marcus ML, Chilian WM, Kanatsuka H, Dellsperger KC, Eastham CL, Lamping KG. Understanding the coronary circulation through studies at the microvascular level. *Circulation.* 1990; 82(1):1–7. [PubMed: 2114232]
19. Masyuk TV, Huang BQ, Masyuk AI, Ritman EL, Torres VE, Wang X, Harris PC, Larusso NF. Biliary dysgenesis in the PCK rat, an orthologous model of autosomal recessive polycystic kidney disease. *Am. J. Pathol.* 2004; 165(5):1719–1730. [PubMed: 15509540]
20. Moghadasali R, Azarnia M, Hajinasrollah M, Arghani H, Nassiri SM, Molazem M, Vosough A, Mohitmafi S, Najarasl M, Ajdari Z, Yazdi RS, Bagheri M, Ghanaati H, Rafiei B, Gheisari Y, Baharvand H, Aghdami N. Intra-renal arterial injection of autologous bone marrow mesenchymal stromal cells ameliorates cisplatin-induced acute kidney injury in a rhesus Macaque mulatta monkey model. *Cytotherapy.* 2014; 16(6):734–749. [PubMed: 24801377]
21. Mori T, Cowley AW Jr. Angiotensin II-NAD(P)H oxidase-stimulated superoxide modifies tubulovascular nitric oxide cross-talk in renal outer medulla. *Hypertension.* 2003; 42(4):588–593. [PubMed: 12975384]
22. Morigi M, Imberti B, Zoja C, Corna D, Tomasoni S, Abbate M, Rottoli D, Angioletti S, Benigni A, Perico N, Alison M, Remuzzi G. Mesenchymal stem cells are renotropic, helping to repair the kidney and improve function in acute renal failure. *J. Am. Soc. Nephrol.* 2004; 15(7):1794–1804. [PubMed: 15213267]
23. Ortiz MC, Garcia-Sanz A, Bentley MD, Fortepiani LA, Garcia-Estan J, Ritman EL, Romero JC, Juncos LA. Microcomputed tomography of kidneys following chronic bile duct ligation. *Kidney Int.* 2000; 58(4):1632–1640. [PubMed: 11012897]
24. Peterson KM, Aly A, Lerman A, Lerman LO, Rodriguez-Porcel M. Improved survival of mesenchymal stromal cell after hypoxia preconditioning: role of oxidative stress. *Life Sci.* 2011; 88(1–2):65–73. [PubMed: 21062632]
25. Pittenger MF, Martin BJ. Mesenchymal stem cells and their potential as cardiac therapeutics. *Circ. Res.* 2004; 95(1):9–20. [PubMed: 15242981]
26. Psaltis PJ, Peterson KM, Xu R, Franchi F, Witt T, Chen IY, Lerman A, Simari RD, Gambhir SS, Rodriguez-Porcel M. Noninvasive monitoring of oxidative stress in transplanted mesenchymal stromal cells. *JACC Cardiovasc. Imaging.* 2013; 6(7):795–802. [PubMed: 23643284]
27. Qian H, Yang H, Xu W, Yan Y, Chen Q, Zhu W, Cao H, Yin Q, Zhou H, Mao F, Chen Y. Bone marrow mesenchymal stem cells ameliorate rat acute renal failure by differentiation into renal tubular epithelial-like cells. *Int. J. Mol. Med.* 2008; 22(3):325–332. [PubMed: 18698491]
28. Qian Q, Li M, Cai Y, Ward CJ, Somlo S, Harris PC, Torres VE. Analysis of the polycystins in aortic vascular smooth muscle cells. *J. Am. Soc. Nephrol.* 2003; 14(9):2280–2287. [PubMed: 12937304]
29. Rangel EB, Gomes SA, Dulce RA, Premer C, Rodrigues CO, Kanashiro-Takeuchi RM, Oskouei B, Carvalho DA, Ruiz P, Reiser J, Hare JM. C-kit(+) cells isolated from developing kidneys are a novel population of stem cells with regenerative potential. *Stem Cells.* 2013; 31(8):1644–1656. [PubMed: 23733311]
30. Rodriguez-Porcel M, Gheysens O, Chen IY, Wu JC, Gambhir SS. Image-guided cardiac cell delivery using high-resolution small-animal ultrasound. *Mol. Ther.* 2005; 12(6):1142–1147. [PubMed: 16111921]

31. Rodriguez-Porcel M, Gheysens O, Paulmurugan R, Chen IY, Peterson KM, Willmann JK, Wu JC, Zhu X, Lerman LO, Gambhir SS. Antioxidants improve early survival of cardiomyoblasts after transplantation to the myocardium. *Mol. Imaging Biol.* 2010; 12(3):325–334. [PubMed: 20013064]
32. Rodriguez-Porcel M, Lerman A, Ritman EL, Wilson SW, Best PJM, Lerman LO. Altered microvascular structure in experimental hypercholesterolemia. *Circulation.* 2000; 102(17):2028–2030. [PubMed: 11044415]
33. Rossetti S, Harris PC. The genetics of vascular complications in autosomal dominant polycystic kidney disease (ADPKD). *Curr. Hypertens. Rev.* 2013; 9(1):37–43. [PubMed: 23971643]
34. Sun N, Lee A, Wu JC. Long term non-invasive imaging of embryonic stem cells using reporter genes. *Nat. Protoc.* 2009; 4(8):1192–1201. [PubMed: 19617890]
35. Swijnenburg RJ, Govaert JA, van der Bogt KE, Pearl JI, Huang M, Stein W, Hoyt G, Vogel H, Contag CH, Robbins RC, Wu JC. Timing of bone marrow cell delivery has minimal effects on cell viability and cardiac recovery after myocardial infarction. *Circ. Cardiovasc. Imaging.* 2010; 3(1):77–85. [PubMed: 19920031]
36. Timmers L, Lim SK, Arslan F, Armstrong JS, Hofer IE, Doevendans PA, Piek JJ, El Oakley RM, Choo A, Lee CN, Pasterkamp G, de Kleijn DP. Reduction of myocardial infarct size by human mesenchymal stem cell conditioned medium. *Stem Cell Res.* 2007; 1(2):129–137. [PubMed: 19383393]
37. Torres VE, Chapman AB, Devuyt O, Gansevoort RT, Grantham JJ, Higashihara E, Perrone RD, Krasa HB, Ouyang J, Czerwiec FS. Tolvaptan in patients with autosomal dominant polycystic kidney disease. *N. Engl. J. Med.* 2012; 367(25):2407–2418. [PubMed: 23121377]
38. Torres VE, Harris PC. Autosomal dominant polycystic kidney disease: the last 3 years. *Kidney Int.* 2009; 76(2):149–168. [PubMed: 19455193]
39. Torres VE, Harris PC. Polycystic kidney disease in 2011: Connecting the dots toward a polycystic kidney disease therapy. *Nat. Rev. Nephrol.* 2012; 8(2):66–68. [PubMed: 22158473]
40. Torres VE, Harris PC. Polycystic kidney disease: genes, proteins, animal models, disease mechanisms and therapeutic opportunities. *J. Intern. Med.* 2007; 261(1):17–31. [PubMed: 17222165]
41. Uchimura H, Marumo T, Takase O, Kawachi H, Shimizu F, Hayashi M, Saruta T, Hishikawa K, Fujita T. Intrarenal injection of bone marrow-derived angiogenic cells reduces endothelial injury and mesangial cell activation in experimental glomerulonephritis. *J. Am. Soc. Nephrol.* 2005; 16(4):997–1004. [PubMed: 15744001]
42. van der Bogt KE, Hellingman AA, Lijkwan MA, Bos EJ, de Vries MR, van Rappard JR, Fischbein MP, Quax PH, Robbins RC, Hamming JF, Wu JC. Molecular imaging of bone marrow mononuclear cell survival and homing in murine peripheral artery disease. *JACC Cardiovasc. Imaging.* 2012; 5(1):46–55. [PubMed: 22239892]
43. Wang D, Iversen J, Wilcox CS, Strandgaard S. Endothelial dysfunction and reduced nitric oxide in resistance arteries in autosomal-dominant polycystic kidney disease. *Kidney Int.* 2003; 64(4):1381–1388. [PubMed: 12969157]
44. Wang D, Strandgaard S, Borresen ML, Luo Z, Connors SG, Yan Q, Wilcox CS. Asymmetric dimethylarginine and lipid peroxidation products in early autosomal dominant polycystic kidney disease. *Am. J. Kidney Dis.* 2008; 51(2):184–191. [PubMed: 18215696]
45. Wang H, Cao F, De A, Cao Y, Contag C, Gambhir SS, Wu JC, Chen X. Trafficking mesenchymal stem cell engraftment and differentiation in tumor-bearing mice by bioluminescence imaging. *Stem Cells.* 2009; 27(7):1548–1558. [PubMed: 19544460]
46. Wang X, Harris PC, Somlo S, Battle D, Torres VE. Effect of calcium-sensing receptor activation in models of autosomal recessive or dominant polycystic kidney disease. *Nephrol. Dial. Transplant.* 2009; 24(2):526–534. [PubMed: 18826972]
47. Warner GM, Cheng J, Knudsen BE, Gray CE, Deibel A, Juskewitch JE, Lerman LO, Textor SC, Nath KA, Grande JP. Genetic deficiency of Smad3 protects the kidneys from atrophy and interstitial fibrosis in 2K1C hypertension. *Am. J. Physiol. Renal Physiol.* 2012; 302(11):F1455–F1464. [PubMed: 22378822]

48. Xu R, Franchi F, Miller B, Crane JA, Peterson KM, Psaltis PJ, Harris PC, Lerman LO, Rodriguez-Porcel M. Polycystic kidneys have decreased vascular density: a micro-CT study. *Microcirculation*. 2013; 20(2):183–189. [PubMed: 23167921]
49. Zhou J, Brugarolas J, Parada LF. Loss of Tsc1, but not Pten, in renal tubular cells causes polycystic kidney disease by activating mTORC1. *Hum. Mol. Genet.* 2009; 18(22):4428–4441. [PubMed: 19692352]
50. Zhu XY, Urbietta-Caceres V, Krier JD, Textor SC, Lerman A, Lerman LO. Mesenchymal stem cells and endothelial progenitor cells decrease renal injury in experimental swine renal artery stenosis through different mechanisms. *Stem Cells*. 2013; 31(1):117–125. [PubMed: 23097349]

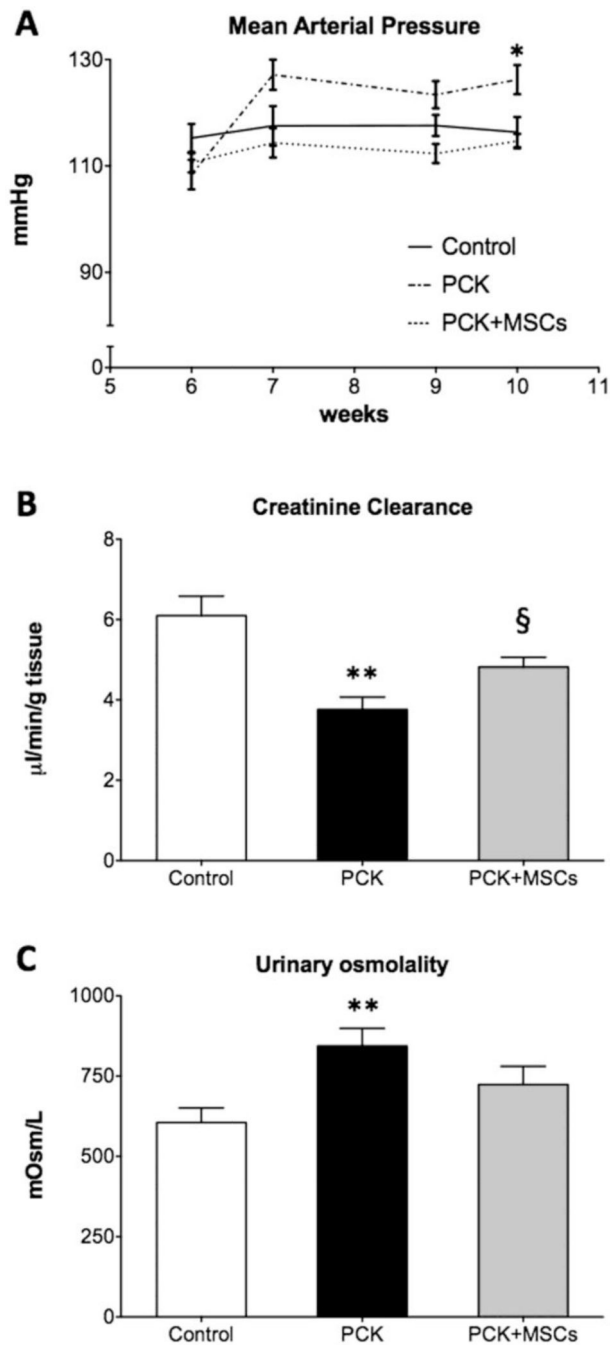


**Figure 1. Blood pressure and renal function of control, PCK and PCK+MSCs animals**  
 Compared to controls, 10 week-old PCK rats had increased SBP (A) with impaired glomerular function, as evidence by a decrease in creatinine clearance (B). PCK animals showed a decrease in urine osmolality (C), compared to controls. A single infusion of MSCs preserved the levels of SBP and improved clinically used parameters of renal glomerular and tubular function. Data represent mean±SEM. \*p<0.05, \*\*p<0.01 vs. control. § p<0.05 vs. PCK. PCK: polycystic kidney disease model, MSCs: mesenchymal stromal cells, SBP: systolic blood pressure.

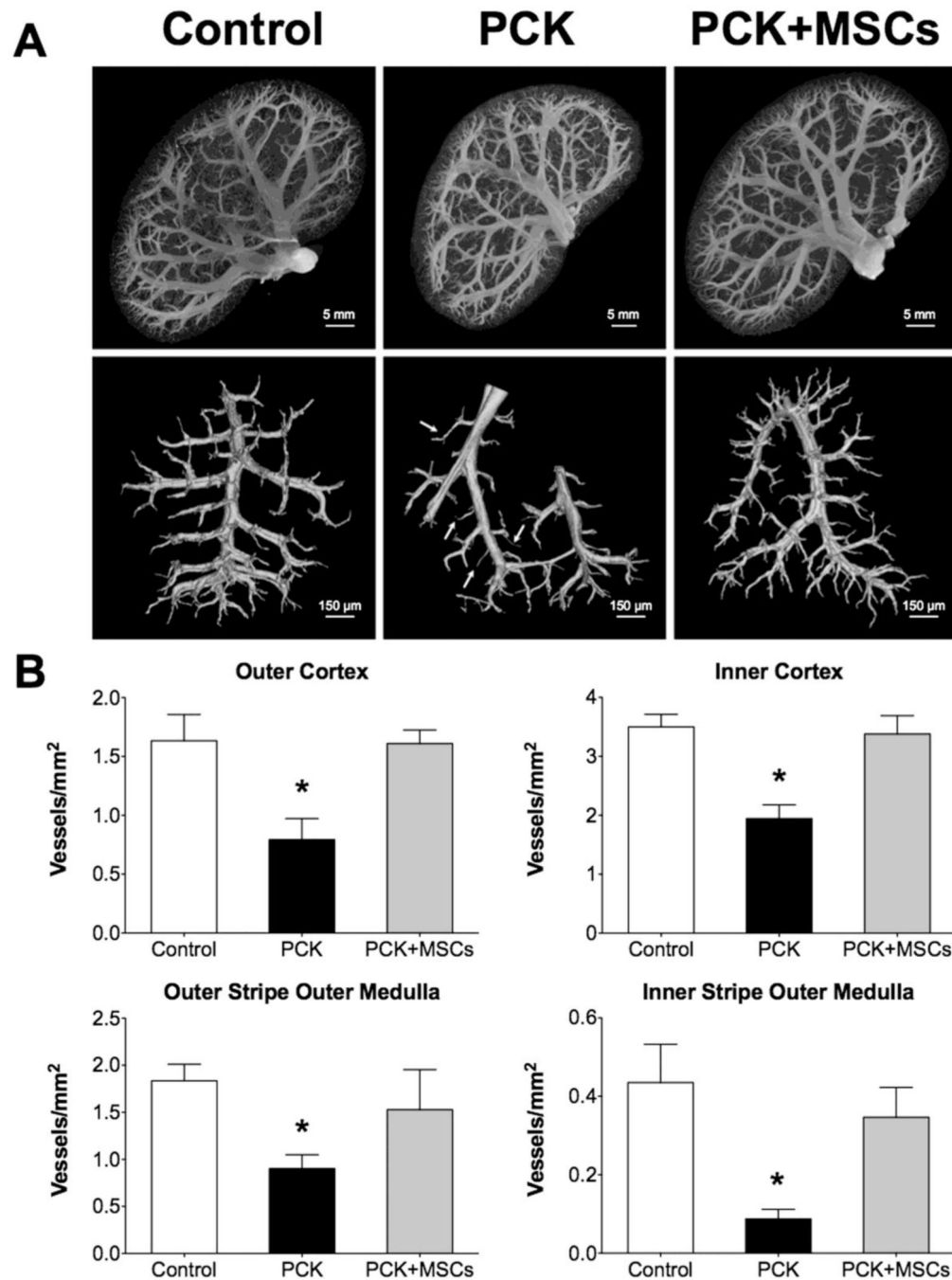


**Figure 2. Vascular analysis using mCT of control, PCK and PCK+MSCs animals**  
 (A) Representative images of kidneys from control, PCK and PCK+MSCs, showing that PKD animals have decreased vascular density, mostly in the cortex, which is normalized after a single infusion of MSCs. (B) cortical (**top**) and medullary (**bottom**) vascular density in all three groups, demonstrating that MSCs had a beneficial effect on both the cortex and the medulla. \* $p < 0.05$  vs. control and PCK+MSCs. mCT: micro computed tomography.

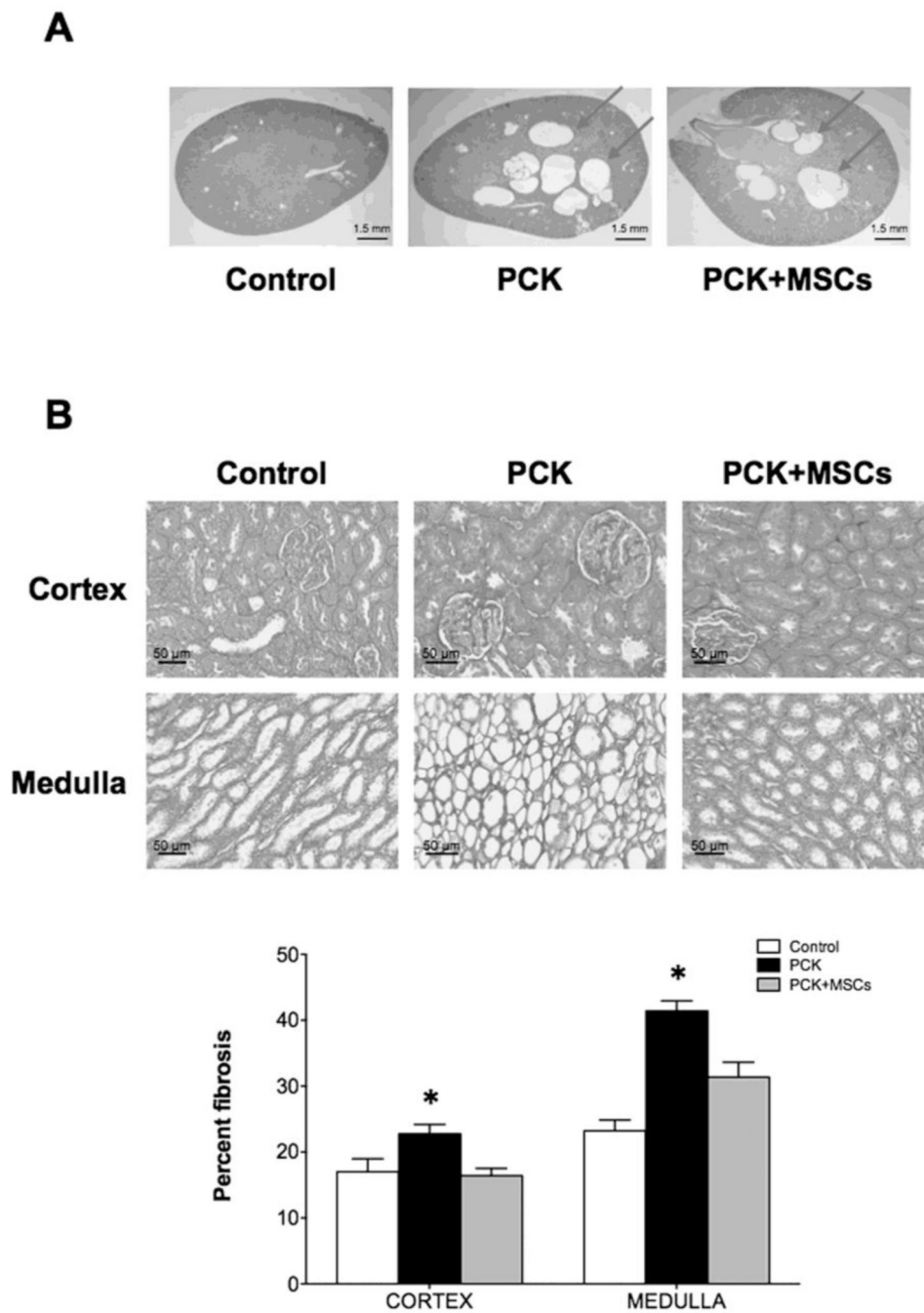


**Figure 3. Histological analysis of control, PCK and PCK+MSCs animals**  
 (A) PCK rats developed cysts that account for  $9.2 \pm 1.8\%$  of the entire kidney area. There was no difference in cyst number or area between the PKD groups. (B) Picosirius red staining (20 $\times$  magnifications) demonstrates increased fibrosis in both the cortex and medulla in PCK rats compared to control and PCK+MSCs rats, quantified as percent of fibrosis. \* $p < 0.05$  vs. control and PCK+MSCs.



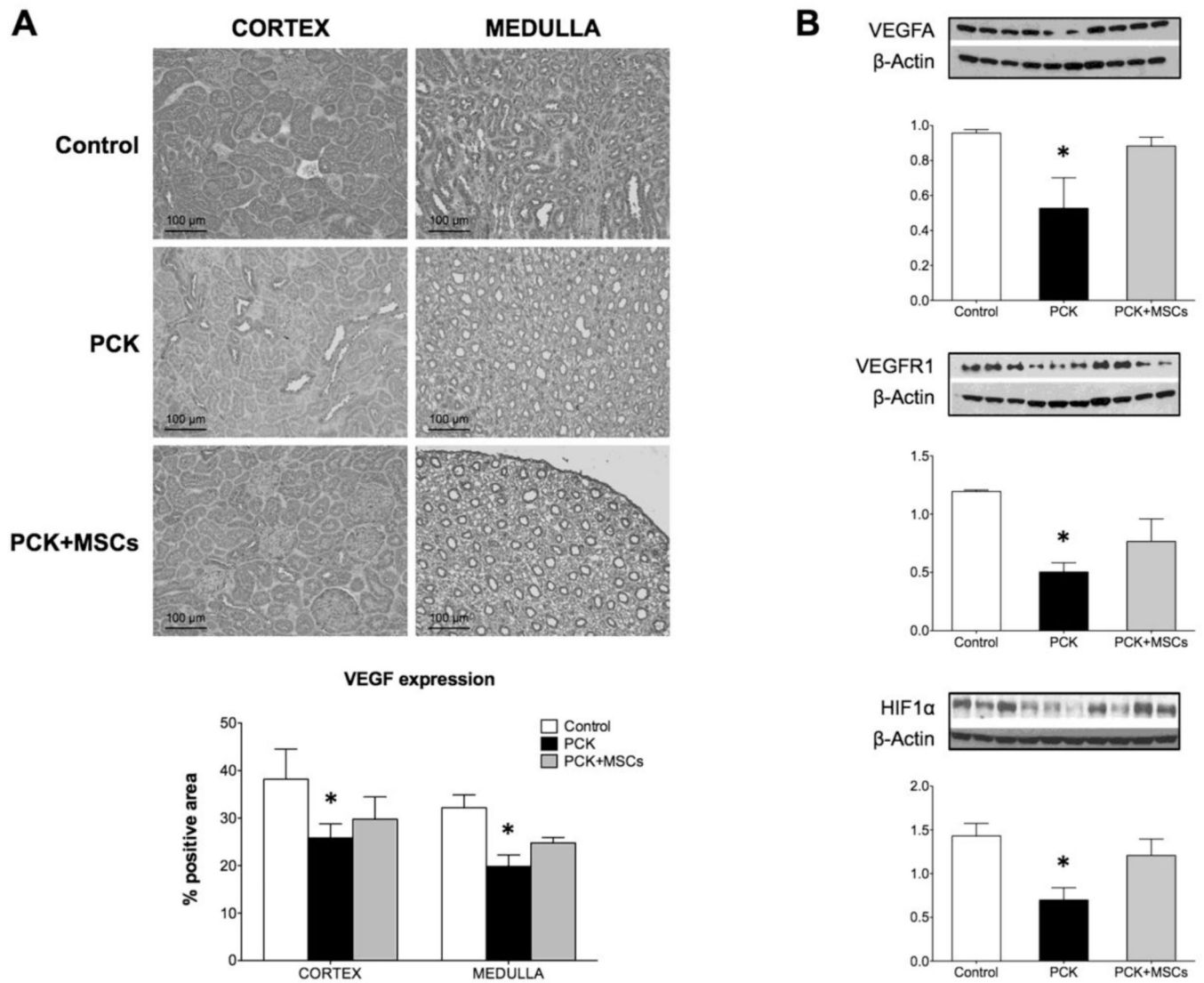


**Figure 4. Analysis of pro-angiogenic cytokines expression**

(A) Representative images of histological staining for VEGFA of renal tissue from control, PCK and PCK+MSCs animals. The quantification, expressed as percentage of positive area, revealed a significantly decreased expression of VEGF in both cortex and medulla, which was improved in the animals that received MSCs. (B) Western Blot analysis of VEGFA, VEGFR1 and HIF1 $\alpha$ , showing that the infusion of MSCs in PCK rats increased the expression of proangiogenic factors. VEGFA: vascular endothelial growth factor A, VEGFR1: VEGF receptor 1, HIF1- $\alpha$ : hypoxia inducible factor 1-alpha. \* $p < 0.05$  vs. control.

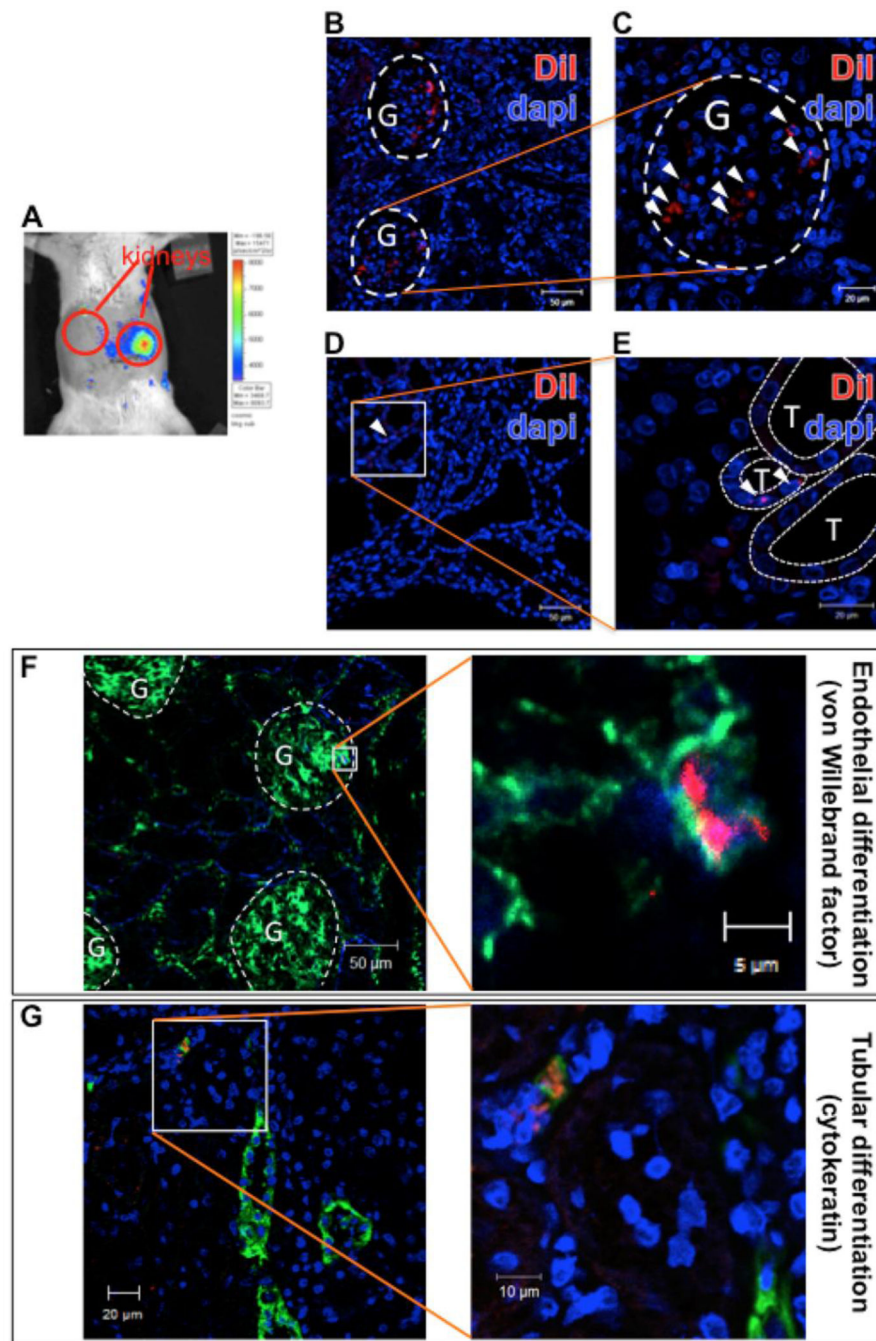


**Figure 5. Engraftment and characteristics of transplanted MSCs**

(A) A representative optical image shows that 1 day after transplantation many of the transplanted MSCs (labeled with firefly luciferase) were present in the infused kidney, and were not observed in the rest of the abdomen areas or the contralateral kidney. (B) At three days post-delivery, most of the infused MSCs, labeled with the fluorescent marker CM-DiI, were detected in the glomeruli (G), outlined with white dashed lines (C, amplification). (D) However, few of them were localized even in the renal interstitial space between tubules (T), outlined with thinner white dashed lines (E, amplification).

Cells remained in the infused kidney as long as four weeks after transplantation. **(F)** Most of the identified MSCs (red) localized in the glomeruli (G, white dashed lines) and expressed the endothelial marker vWf (green), suggesting that they acquired certain characteristics of endothelial phenotype. **(G)** Moreover, some MSCs that were detected in the renal interstitial space, co-localized with the epithelial (tubular) marker pan-cytokeratin (green). vWF: vonWillebrand factor.

Author Manuscript

Author Manuscript

Author Manuscript

Author Manuscript

**Table**

Quantitation of renal vasculature assessed by mCT in Control, PCK and PCK+MSCs rats.

		<b>Control</b>	<b>PCK</b>	<b>PCK+MSCs</b>
<b>Cortical vascular density (per cm<sup>2</sup>)</b>	<i>14–199<math>\mu</math>m</i>	369 $\pm$ 40	157 $\pm$ 45*	369 $\pm$ 21
	<i>&gt;200<math>\mu</math>m</i>	260 $\pm$ 6	220 $\pm$ 7*	320 $\pm$ 6
<b>Vascular Volume Fraction (%)</b>	<i>Outer cortex</i>	21.83 $\pm$ 1.02	21.03 $\pm$ 1.7	22.62 $\pm$ 1.69
	<i>Inner cortex</i>	24.82 $\pm$ 1.50	20.82 $\pm$ 1.32*	23.90 $\pm$ 1.87
	<i>Outer strip outer medulla</i>	21.91 $\pm$ 0.62	19.22 $\pm$ 1.46 <sup>¥</sup>	19.25 $\pm$ 1.80 <sup>¥</sup>
	<i>Inner strip outer medulla</i>	25.59 $\pm$ 1.34	18.01 $\pm$ 0.54 <sup>¥</sup>	17.93 $\pm$ 1.50 <sup>¥</sup>
<b>Glomeruli</b>	<i>Total number</i>	26,957 $\pm$ 2,659	29,638 $\pm$ 6,328	23,802 $\pm$ 2,171
	<i>Glomerular diameter (<math>\mu</math>m)</i>	127 $\pm$ 2	145 $\pm$ 5*	129 $\pm$ 3

\* p&lt;0.05 compared to control and PCK+MSCs,

<sup>¥</sup> p<0.05 vs. control

PCK: polycystic kidney disease model

MSCs: mesenchymal stromal cells